

# Evaluation of Temperature Effects for Quantum Cascade Laser Dynamics (QCLs)

Mushtaq O. Oleiwi<sup>1,\*</sup>, Dhiaa Jabbar Akoosh<sup>2</sup> and Sadeq Kh. Ajeel<sup>3</sup>

<sup>1</sup>Department of Physics, College of Education for Pure Sciences, University of Thi-Qar, Thi-Qar, 64001, Iraq

<sup>2</sup>General Directorate of Education in Dhi Qar. Dhi Qar, Iraq

<sup>3</sup>Department of Physics, College of Sciences, University of Thi-Qar, Nasiriyah, Iraq

Received: 12 Mar. 2023, Revised: 12 Apr. 2023, Accepted: 22 Apr. 2023

Published online: 1 May 2023

**Abstract:** We introduce a 3-level rate equation approach to modelling a rate equation model for the dynamics of quantum cascade (QCLs) lasers that is based on cascaded active regions. We analyze the evolution of output and carrier numbers at each level taking into account temperature, the effect of the cavity widths, and the specified parameters (injection current density, confinement factor). This leads to an increase in output photons and carrier numbers.

**Keywords:** QCL, Dynamics, Temperature, Gain, Lifetimes.

## 1 Introduction

The pulse emission outputs of the quantum cascade lasers are currently greater than one Watt, and they function at high temperatures [1-3]. They are coherent radiation sources that are electrically driven. Another possible continuous-wave source with mediocre thermal performance is the quantum cascade laser (QCL)[3-5]. It has been shown that low temperatures are the most practical operating temperature for continuous waves. The equivalent output power soon decreases as the temperature rises because the provider dynamics are temperature-sensitive. Therefore, it is crucial to comprehend and take into account how the temperature dependence of carrier dynamics affects the behavior of lead QCLs. The time-domain conduct of modulated THz QCLs is also significant. THz QCLs may outperform diodes in terms of high-speed dynamic performance due to the absence of rest oscillations. However, the frequently used REs models[11,12] treat the laser's three key parameters—carrier lifetimes, gain, and injection current—as constants that are unaffected by bias or temperature. Because of this, these models are only accurate at or close to the bias and temperature for which the parameters have been determined [15-17]. The goal of this work is to better understand QCL

dynamics, an area where this laser has several novel applications. This study explores the effects of cavity size, output photon gain, electron count, durations for level transitions, and electron number on resonator stability.

## 2 Rate equations for QCL

Since a four-level QC laser is frequently used in the literature [16,18], that is what we will concentrate on. The upper and lower states will be referred to as levels 3 and 2, respectively, while the ground state, which is utilized to empty the lower state, will be referred to as stage 1. A schematic of the three-level electrical system used by the QCLs is shown in Fig. 2. Because of the population inversion between laser levels 3 and 2, stimulated emission is practical [19].

\*Corresponding author E-mail: mushtagobaid@utq.edu.iq

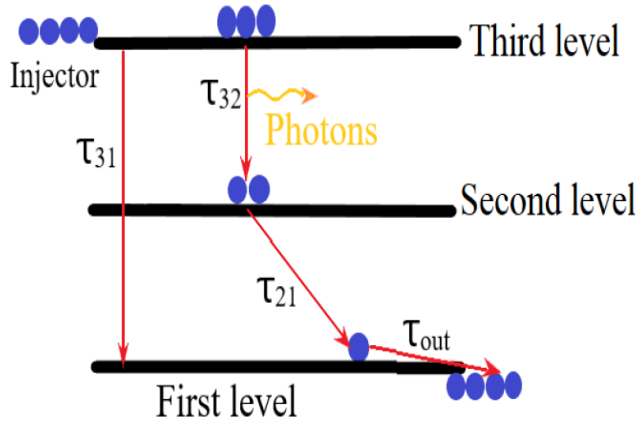


**Fig. 1:** Assignment of three electronic levels for QCLs [19].

The following charge equations are provided by [16,17] and represent  $N_1$ ,  $N_2$ , and  $N_3$  as the instantaneous numbers of electrons in each of the three levels and the cavity's photon number, respectively.

$$\frac{dN_3}{dt} = WL \frac{J}{e} - \frac{N_3}{\tau_3} - \Gamma \frac{c' \sigma_{32}}{V} (N_3 - N_2) N_{ph}, \quad (1)$$

$$\frac{dN_2}{dt} = \left( \frac{1}{\tau_{32}} + \frac{1}{\tau_{sp}} \right) N_3 - \frac{N_2}{\tau_{21}} + \Gamma \frac{c' \sigma_{32}}{V} (N_3 - N_2) N_{ph}, \quad (2)$$

$$\frac{dN_1}{dt} = \frac{N_3}{\tau_{31}} + \frac{N_2}{\tau_{21}} - \frac{N_1}{\tau_{out}}, \quad (3)$$

$$\frac{dN_{ph}}{dt} = \Gamma \frac{c' \sigma_{32}}{V} (N_3 - N_2) N_{ph} + N \beta \frac{N_3}{\tau_{sp}} - \frac{N_{ph}}{\tau_p}. \quad (4)$$

In the above system of equations,  $J$  denotes the electron current density that tunnels into the upper level and  $e$  is the electronic charge,  $\beta$  is spontaneous emission factor, while  $W$  and  $L$  are the lateral dimensions of the cavity.  $W$  and  $L$  width of each one of these, the whole volume  $V$  of the active area. In addition, in the above equations one introduced the mode confinement factor  $\Gamma$  and the average velocity of light in the system  $v_g$  given by  $v_g = c / n_{eff}$ , where  $n_{eff}$  and  $c$  are the effective refractive index of the cavity and the speed of light in vacuum, respectively [18-20]. whereas  $\tau_{32}$  stands for the stimulated emission cross section between the upper and lower levels [20-23]. The system dynamics is mainly determined by the three non-

radiative scattering times denoted by  $\tau_{32}$ ,  $\tau_{31}$ , and  $\tau_{21}$  that are due to LO-phonon emission between the corresponding levels as well as the radiative spontaneous relaxation time  $\tau_{sp}$  between levels 3 and 2.

The relation between current density and temperature is given by [16,17]:

$$J_{th} = J_o \exp(T / T_o)$$

where  $J_o$  is the threshold current density at 300K and  $T_o$  is the characteristic temperature.

$$G(N, P) = \Gamma_z a_N \log \frac{N}{N_0}$$

Where  $\Gamma_z$  is the longitudinal confinement factor,  $a_N$  is the gain parameter and  $N_0$  is the carrier concentration at transparency.

### 3 Results

We can be solved the rate equations of QCL by matlab program (ode45 method) with initial conditions for numbers for photons and carriers for each level.

We estimate numerically,  $J_{th} = 2.6 \text{ kA/cm}^2$  and ( $J = 2 \text{ Jth}$ ). QC laser parameters are used [17]:  $W = 34 \text{ }\mu\text{m}$ ,  $L = 1 \text{ mm}$ ,  $\Gamma = 0.32$ ,  $m = 20$ ,  $n_{eff} = 3.27$ ,  $\tau_{32} = 2.1 \text{ ps}$ ,  $\tau_3 = 1.4 \text{ ps}$  and  $\tau_{21} = 0.3 \text{ ps}$ ,  $\tau_{31} = 2.6 \text{ ps}$ ,  $\beta = 1 \times 10^{-4}$ ,  $\tau_{sp} = 38 \text{ ns}$ ,  $\tau_p = 3.36 \text{ ps}$  and  $\sigma_{32} = 1.8 \times 10^{-14} \text{ cm}^2$ .

#### 3.1. Effect of current injection density

Figure (2) depicts the time development of the QC laser's photon output at various injection current densities ( $J$ ).

The temporal development of the number of electrons in the level 3 of the QC laser at various injection current densities ( $J$ ) is shown in Figure 3.

The temporal development of the quantity of electrons in the level 2 of the QC laser at various injection current densities ( $J$ ) is shown in Figure (4).

The temporal development of the number of electrons in the level 1 of the QC laser at various injection current densities ( $J$ ) is shown in Figure (5).

As seen in figure (2), the photon count increases as the injection current density increases. The cause of this effect results from an increase in carrier injection, which raises the number of carriers and satisfies the gain for photons.

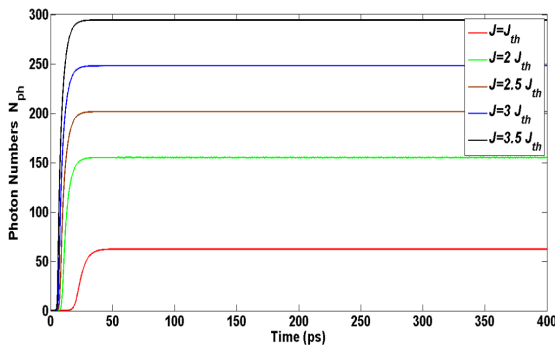


**Fig.2:** Time evolution of the number of photons of the QC laser under different injection current densities ( $J$ ).

We see that the number of carriers increases together with the increase in injection current density, satisfying rising ( $N_3$ ,  $N_2$  and  $N_1$ ) in figures. (3, 4, and 5).

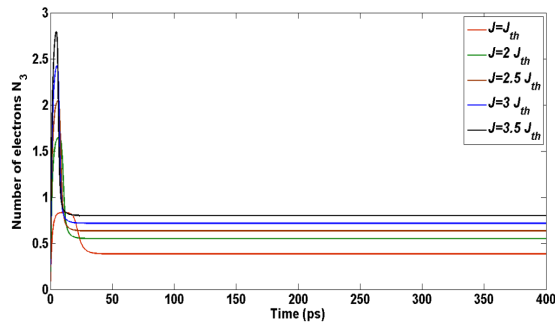


**Fig.3:** Time evolution of the number of electrons in the level 3 of the QC laser under different injection current densities ( $J$ ).

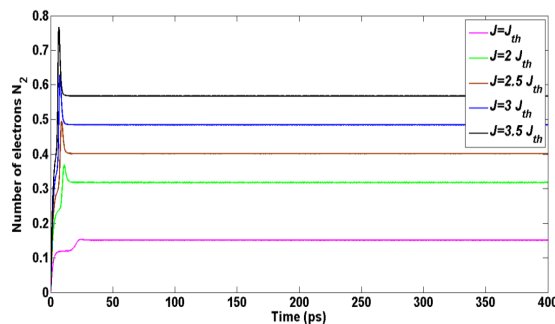


**Fig.4:** Time evolution of the number of electrons in the level 2 of the QC laser with different injection current densities ( $J$ ).

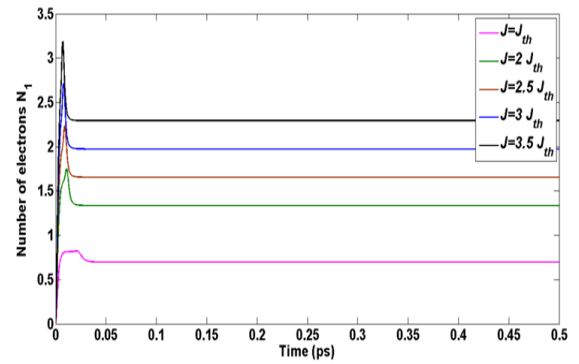


**Fig. 5:** Time evolution of the number of electrons in the level 1 of the QC laser with different injection current densities ( $J$ ).

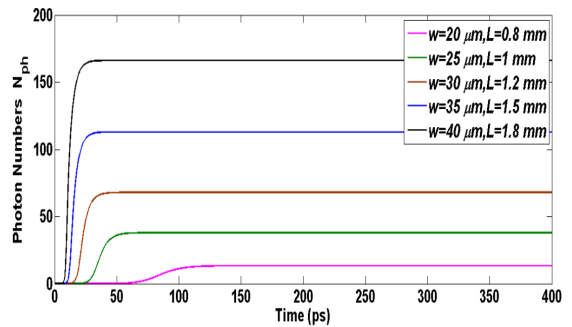


**Fig. 6:** Time evolution of the number of photons of the QC laser with different values of widths ( $W,L$ ).

### 3.2. Effect of cavity widths ( $W,L$ ):

The temporal development of the QC laser's photon count at various widths ( $W,L$ ) is seen in Figure 6. Figure (7) depicts the change in the quantity of electrons over time for the QC laser's level 3 at various widths ( $W,L$ ). The temporal development of the quantity of electrons for level 2 of the QCL laser for various widths ( $W,L$ ) is shown in Figure (8).

Figure (9) depicts the temporal evolution of the number of electrons for QC laser level 1 at various widths ( $W,L$ ).

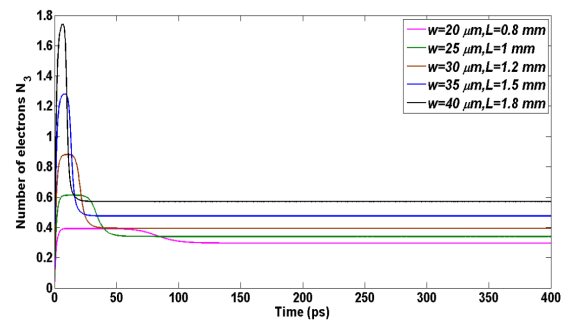


**Fig. 7:** Time evolution of the number of electrons for level 3 of the QC laser under different values of widths ( $W, L$ ).

We see that increasing cavity length and breadth has an impact on the dynamics of level 3 ( $N_2$ ) electrons, as illustrated in figure (8), where the electron number grew and the switch-on time decreased. We see that the dynamics of

the level 3 (N3) electrons are affected by the growing cavity length and breadth, as illustrated in figure (7), where the electron number grew and the switch on time decreased.

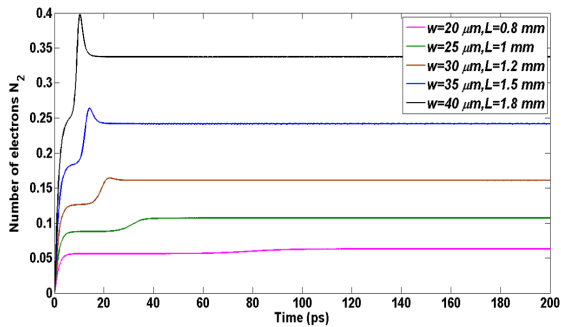


**Fig. 8:** Time evolution of the number of electrons for level 2 of the QC laser under different values of widths (W,L).

As shown in figure (9), when the quantity of electrons increased and the switch-on duration reduced, we can observe that the dynamics of the level 3 (N1) electrons are impacted by the expanding cavity length and width. The variation in cavity diameters has an effect on population inversion.

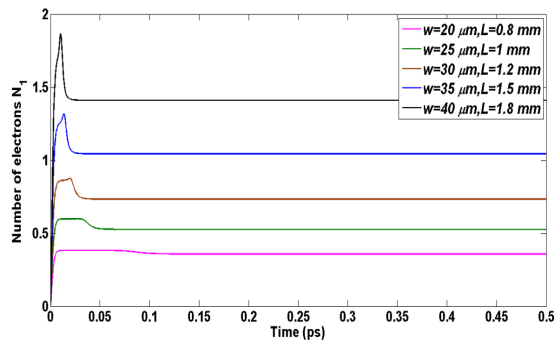


**Fig. 9:** Time evolution of the number of electrons for level 1 of the QC laser under different values of widths (W,L).

The dynamics of QCLs are affected by increasing the confinement factor  $\Gamma$  which leads to increasing the photon output (photon number  $N_{ph}$ ), because this parameter determines the carriers, thus these increasing leads to photon number increasing as shown in figure (10).

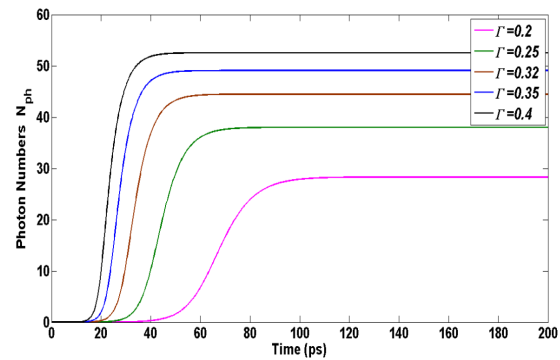


**Fig. 10:** Time evolution of the number of photons of the QC laser different values of confinement factor.

### 3.3. Effect of confinement factor:

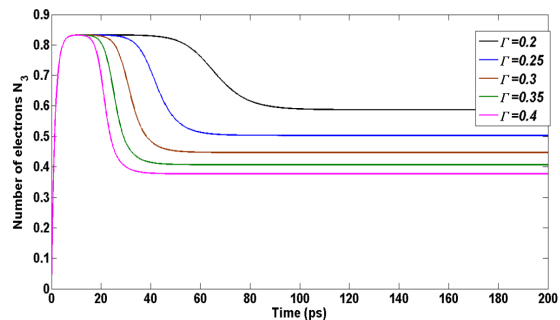
Figure(10) depicts a time series of the quantity of photons  $p$  produced by the QC laser at various confinement factor level  $s$ .

Figure (11) depicts the time development of the number of electrons for the QC laser's level 3 at various confinement  $f$  factor values.

Figure (12) depicts a time series of the number of electrons at level 2 of the QC laser at various confinement factor values.

Figure(13) depicts a time history of the number of electrons at various confinement factor values for the QC laser's level 1 operation.

Due to the fact that this parameter influences the carriers, raising the confinement factor has an impact on the dynamics of QCLs and results in an increase in (electron number  $N_3$  in level 3).



**Fig. 11:** Time evolution of the number of electrons for level 3 of the QC laser different values of confinement factor.

Raising the confinement factor has an effect on the dynamics of QCLs and causes a rise in the electron number ( $N_2$  in level 2), as shown in figure (12), since this parameter affects

the carriers.

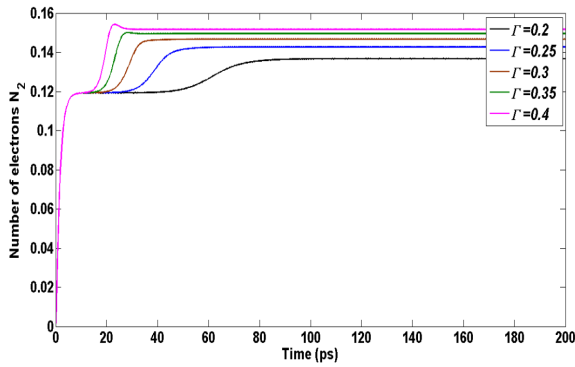


**Fig. 12:** Time evolution of the number of electrons for level 2 of the QC laser different values of confinement factor.

Raising the confinement factor has an impact on QCL dynamics and raises (electron number  $N_1$  in level 1) because the se increases result in a rise in the number of electrons, as shown in figure (13), since this parameter affects the carriers.

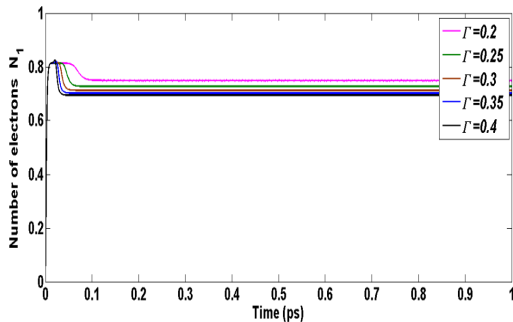


**Fig. 13:** Time evolution of the number of electrons for level 1 of the QC laser different values of confinement factor.

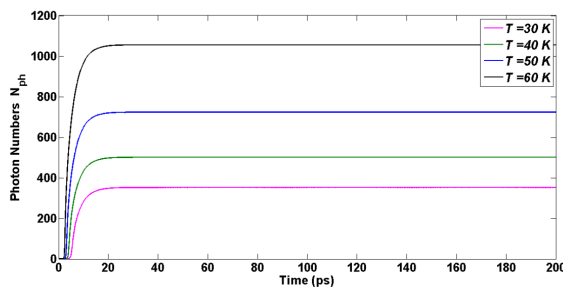
### 3.4. Effect of temperature:

Figure (14), which depicts the temporal behavior of the QC laser's photon number at various temperatures.

Figure (15) depicts the temporal behavior of the number of electrons at level 3 of the QC laser at various temperatures.

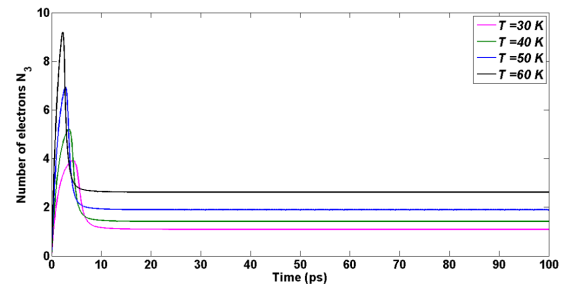
Figure (16) depicts the temporal behavior of the number of electrons at level 2 of the QC laser at various temperatures.

Figure (17) depicts the temporal behavior of the number of electrons at the QC laser's level 1 at various temperatures.



**Fig. 14:** Time evolution of the number of photons of the QC laser different values of temperatures.

The dynamics of QCLs are affected by increasing the  $T$  which leads to increasing (electron number  $N_3$  in level3), because this parameter determines the carriers, thus these increasing leads to electron number increasing as shown in figure (15).



**Fig. 15:** Time evolution of the number of electrons for level 3 of the QC laser different values of temperature.

Since this parameter influences the carriers, raising the  $T$  has an impact on the dynamics of QCLs and results in an increase in (electron number  $N_2$  in level2), as seen in figure 16.

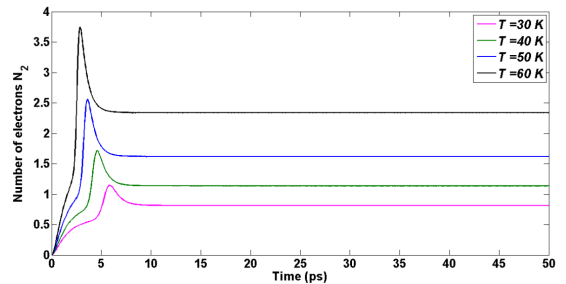


**Fig. 16:** Time evolution of the number of electrons for level 2 of the QC laser different values of temperature.

The dynamics of QCLs are affected by increasing the  $T$  which leads to increasing (electron number  $N_1$  in level1), because this parameter determines the carriers, thus these increasing leads to electron number increasing as shown in figure (17).

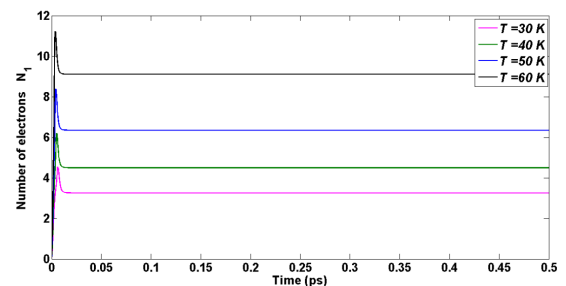


**Fig. 17:** Time evolution of the number of electrons for level 1 of the QC laser different values of temperature.

## 4 Conclusions

The dynamics of a three-level QC laser were explored using a straightforward rate equations model, and it was discovered that the injection current played a significant influence in determining, among other things, how photons and carriers behaved. We also provided an analytical explanation of how temperature increases affect system dynamics. Our numerical findings also demonstrate how, for each level, the behavior of photons and carriers is changed as cavity widths increase. The relevance of length and width in the under investigation QCL structure. As length and width varies, the threshold current and temperature are affected.

The value of length and width in the QCL structure that is the subject of this inquiry.

The dynamics of photons and electrons are affected by variations (increasing) in cavity dimensions as well as threshold current, confinement factor, and temperature.

## Acknowledgements

The authors would like to thank Dr. Amin H. Al-Khursan for his help in reading the results and making comments.

## References

- [1] Y. Ren, R. Wallis, D. S. Jessop, R. Degl'Innocenti, A. Klimont, H. E. Beere, and D. A. Ritchie, *Appl. Phys. Lett.*, **107**, 011107(2015).
- [2] L. H. Li, L. Chen, J. R. Freeman, M. Salih, P. Dean, A. G. Davies, and E. H. Linfield, *Electron. Lett.*, **53(12)**, 799 (2017).
- [3] L. Bosco, M. Franckie, G. Scalari, M. Beck, A. Wacker, and J. Faist, *Appl. Phys. Lett.*, **115**, 010601(2019).
- [4] L. Consolino, S. Bartalini, H. E. Beere, D. A. Ritchie, M. S. Vitiello, and P. De Natale, *Sensors*, **13**, 3331(2013).
- [5] Chan C. W. I., "Towards Room-Temperature Terahertz Quantum Cascade Lasers: Directions and Design", Massachusetts Institute of Technology, PhD Theses and Dissertations., (2015).
- [6] A. D. Rakic', T. Taimre, K. Bertling, Y. L. Lim, P. Dean, A. Valavanis, and D. Indjin, *Appl. Phys. Rev.*, **6**, 021320(2019).
- [7] T. Nagatsuma, G. Ducournau, and C. C. Renaud, *Nat. Photonics* **10**, (2016) 371.
- [8] Hillbrand, J.; Andrews, A.M.; Detz, H.; Strasser, G.; Schwarz, B. Coherent injection locking of quantum cascade laser frequency combs. *Nat. Photon.*, **13**, 101–104(2018).
- [9] Bachmann, D.; Rösch, M.; Süess, M.J.; Beck, M.; Unterrainer, K.; Darmo, J.; Faist, J.; Scalari, G. Short pulse generation and mode control of broadband terahertz quantum cascade lasers. *Optica*, **3**, 1087(2016).
- [10] Y. Zeng, B. Qiang, and Q. J. Wang, *Adv. Opt. Mater.*, **8**, 1900573(2020).
- [11] I. Kundu, J. R. Freeman, P. Dean, L. Li, E. H. Linfield, and A. G. Davies, *ACS Photonics*, **7**, 765(2020).
- [12] I. Kundu, J. R. Freeman, P. Dean, L. H. Li, E. H. Linfield, and A. G. Davies, *Opt. Express*, **28**, 4374(2020).
- [13] G. Liang, Y. Zeng, X. Hu, H. Yu, H. Liang, Y. Zhang, L. Li, A. G. Davies, E. H. Linfield, and Q. J. Wang, *ACS Photonics*, **4**, 517 (2017).
- [14] C. A. Curwen, J. L. Reno, and B. S. Williams, *Appl. Phys. Lett.* **113**, (2018) 011104.
- [15] L. Xu, D. Chen, T. Itoh, J. L. Reno, and B. S. Williams, *Opt. Express*, **24**, 24117(2016).
- [16] H. Page, C. Becker, A. Robertson, G. Glastre, V. Ortiz, and C. Sirtori, *Appl. Phys. Lett.*, **78**, 3529 (2001).
- [17] W. H. Ng, E. A. Zibik, M. R. Soulby, L. R. Wilson, J. W. Cockburn, H. Y. Liu, M. J. Steer, and M. Hopkinson, *J. Appl. Phys.*, **101**, 046103(2007).
- [18] G. Scamarcio, F. Capasso, C. Sirtori, J. Faist, A. L. Hutchinson, D. L. Sivco, and A. Y. Cho, *Science*, **276**, 773(1997).
- [19] Wang X. G., Grillot F. and Wang C., "Rate equation modeling of the frequency noise and the intrinsic spectral linewidth in quantum cascade lasers", *Opt. express*, **26**, 002325-002334 (2018).
- [20] D. Hofstetter, M. Beck, T. Aellen, and J. Faist, *Appl. Phys. Lett.* **78**(2001) 396.
- [21] J. Faist, M. Beck, T. Aellen, and E. Gini, *Appl. Phys. Lett.*, **78**, 147(2001).
- [22] C. Walther, G. Scalari, J. Faist, H. Beere, and D. Ritchie, *Appl. Phys. Lett.*, **89**, 231121(2006) .
- [23] A. Hamadou, J.-L. Thobel, and S. Lamari, *Opt. Commun.* **281**, 5385(2008).